Korean J. Chem. Eng., **30**(4), 823-830 (2013)
DOI: 10.1007/s11814-012-0233-9

Viscous dissipation effect on heat transfer characteristics of mixed electromagnetic/pressure driven liquid flows inside micropumps

Mostafa Shojaeian*,† and Seyyed Mohammad Nima Shojaee**

*Mechatronics Engineering Program, Faculty of Engineering and Natural Sciences, Sabanci University, Tuzla, Istanbul 34956, Turkey
**Department of Mechanical and Aerospace Engineering, Science and Research Branch, Islamic Azad University, Tehran, Iran
(*Received 23 September 2012 • accepted 20 December 2012*)

Abstract−This paper presents the effect of viscous dissipation on heat transfer characteristics of mixed electromagnetic/pressure driven liquid slip flows inside parallel plate microchannels. Flow is governed by the Navier-Stokes equations subject to the imposition of electromagnetic field with the boundary condition appropriate to the slip flow regime. For isoflux walls, some closed form expressions for the local and bulk temperature profiles and the Nusselt number in terms of dimensionless slip length, Hartmann number and Brinkman number are given, while the viscous dissipation is also taken into account. Then the analytical solutions derived in this analysis are elaborated. It turns out that since the contribution of the viscous dissipation on the Nusselt number under the given circumstances, especially a stronger electromagnetic field, may reach to nearly 10%, therefore, the viscous heating should be taken into consideration. Otherwise, the heat transfer rate may be overestimated or underestimated depending on whether the fluid is being heated or cooled. Also, there are singularities in Nusselt number values, which move close together by including the viscous dissipation. Further, an increase in the Hartmann number increases the convection, which is especially reflected in smaller values of dimensionless slip length.

Key words: Microchannel, Liquid Slip Flow, Electromagnetic Field, Nusselt Number, Viscous Dissipation

INTRODUCTION

Recent progress in micro-fabrication techniques for micro-fluidic systems and in methods for the analysis of micro-fluid devices have made it possible to design complex micro-fluidic devices such as lab-on-chip, fuel cell, heat exchanger and so on. To apply these micron-sized devices, one should have a fundamental knowledge of micro-channels where the continuum assumption is no longer valid and the Navier-Stokes equations must be solved in conjunction with velocity-slip and temperature-jump at walls. There are many experimental works (for example, see reviews [1-3]), highlighting that the deviations from conventional theory in experimental results for laminar flow through microchannels were attributed to the size of the channels.

Several researchers addressed slip length for liquid microflows. For instance, the slip length ranging 6-8 μm was evaluated by Chun and Lee [4], inferring from the experimental results of dilute colloidal suspension in a slit-like channel. Joseph and Tabeling [5] measured the slip length of water flowing through thin microchannels and found that it is within ±100 nm. Tretheway and Meinhart [6] also found that the slip length of water flow in a 30×300 μm channel coated with a monolayer is nearly 1 μm.

Many numerical and analytical solutions, being gas or liquid, are also available in the literature; for example, refer to [7-12]. Their results confirm that the inclusion of velocity-slip and temperature-jump conditions leads to a change in the heat transfer and fluid flow characteristics so that they can match experimental measurements.

Viscous dissipation influences are normally significant for high viscous flows (such as liquid flows) or high velocity gradients in macroscales, while it becomes significant even for typical flows in microscales. Accordingly, viscous dissipation should be taken into account to avoid incorrect results in microchannels. It is introduced in the energy equation as a source term and effectively influences convective heat transfer in some cases by changing temperature distribution. Several researchers, showing that viscous heating plays an important role in convection [13-20], have reported its effect on the heat transfer rate for microchannels under slip/jump boundary conditions.

On the other hand, magneto-hydrodynamic (MHD) flows relevant to macroscales have been investigated in some references such as [21-24]. Andreev et al. [25] conducted an experimental study of a turbulent liquid metal flow in a rectangular minichannel under the influence of an inhomogeneous magnetic field, which is a basic problem of liquid metal magnetohydrodynamics pertinent to the technique of electromagnetic braking in the process of continuous casting of steel as well as for Lorentz force velocimetry. A number of Plexiglas blocks tightly covered the top channel in order to make sure no-slip boundary conditions. They placed two finite permanent magnets coupled by a steel yoke at outside the central part of the channel. With the insulating walls, an induced electric field was measured due to the interaction between convective terms (because of the turbulent flow) and the magnetic field. In a further work [26], they applied an ultrasonic velocity profile (UVP) method to a similar problem. Chen et al. [27] conducted MHD experimental design and program for Chinese liquid metal LiPb experimental loop DRAGON-IV and analyzed the performance of MHD flow characteristics.

In recent decades, micropumps in mechanical and non-mechanical forms are typically used to drive small volume of fluid in microchannels. Moreover, the advent of magnetohydrodynamic micro-

†To whom correspondence should be addressed.
E-mail: shojaeian@sabanciuniv.edu, mostafa_shojaeian@yahoo.com

pumps (or magnetohydrodynamic in microchannel) has attracted researchers to study problems based on microfluidics due to its various applications. It works based on Lorentz Force, which is generated by applying an electric field to the conductive fluid across the channel along with a perpendicular magnetic field. For flow through magnetohydrodynamic micropumps, some works with the assumption of non-slip condition can be found in the literature [28-31].

Siegel et al. [32] explained a method for fabrication of complex metallic microstructures in 3D by injecting liquid solder into microfluidic channels, and allowing the solder to cool and solidify. Employing liquid metals with high conductivity enables Hartman number to increase. Their method significantly can facilitate the way for fabricating metallic wires, electrodes, electromagnets, or heating elements relevant to microfluidic channels (<10 μm) (see also Ref. [33]). In spite of using mercury for MHD actuation, the accessibility of other liquid metals and metal alloys with low melting temperature would let utilizing liquid metals in microchannels. Dickey et al. [34] also studied the behavior of the electrically conductive fluid metal eutectic, injecting into microfluidic channels at room temperature. *EGaIn* and *Hg* were brought into the microchannel by applying pressure to the inlet using regulated pressurized nitrogen, while the outlet was at atmospheric pressure. Qian and Bau also presented a comprehensive review on MHD-based microfluidics [35].

However, microscale study of MHD flows subject to slip conditions is scarce and it has been recently put into investigation. With regard to this, the steady state, incompressible, MHD Couette rarefied flows inside two conducting walls was examined by Soundalgekar [36,37] who fulfilled the magnetic induction as well as the slip condition and then obtained the velocity distributions. He did a further study in which an expression for Nusselt number for parallel plate microchannel was derived by implementing the slip/jump boundary conditions at walls in addition to assuming a transversely uniform magnetic field and neglecting advection term [38]. Cai and Liu [39] investigated low-magnetic-Reynolds-number compressible gas flows inside a two-dimensional microchannel. Their asymptotic solution led to obtain the velocities, pressure, and temperature distributions with the assumptions of quasi-isothermal and slip/jump boundary conditions at walls.

Actually, this work is a natural extension from the recent paper [40] in which the fluid flow and heat transfer characteristics of mixed electromagnetic/pressure driven slip flows within microchannels in the case of isoflux walls were analyzed without viscous dissipation effect included. Since viscous heating effect may strongly affect convection, and seemingly, there is a lack of information about flow characteristics of a viscous dissipative electromagnetohydrodynamic liquid slip flows. Therefore, the aim of this study is to find its effect on the convective heat transfer within parallel plate microchannels with isoflux walls and to acquire corresponding expression for the Nusselt number.

PROBLEM DESCRIPTION

Hydro-dynamically and thermally, fully developed laminar flow of an electrically conducting fluid exposed to the electromagnetic field inside parallel plate microchannels with isoflux walls is theoretically studied in this paper. Compared to Ref. [40], the viscous dissipation by employing a different dimensionless temperature is included. That is, the flow is considered to be steady, incompressible with constant properties in which a constant external magnetic field at a value B in the Y direction is applied, while a constant electrical field in Z-direction is induced as a result of a potential difference via electrodes (i.e., $E_x=E_y=0$), see Fig. 1. The magnetic Reynolds number, $Re_m=\sigma\mu_m U_m L$, is very small, indicating that the flow of an electrically conducting fluid does not change the magnetic field. Therefore, the induced magnetic field is neglected in the paper to avoid complexity of the solution [41].

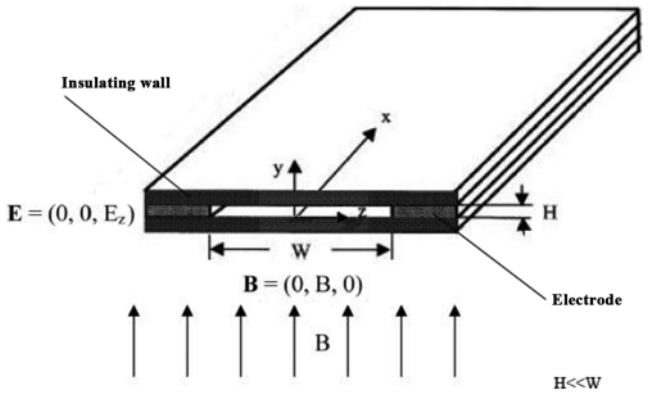

Fig. 1. A schematic of the channel, B=(0, B, 0) and E=(0, 0, E_z).

When $Re_m \ll 1$, the electric field may be obtained from a scalar potential,

$$E=-\nabla\phi \tag{1}$$

and current may be computed using Ohm's law:

$$\vec{J}=\sigma(-\nabla\phi+\vec{V}\times\vec{B}) \tag{2}$$

The electric potential is derived by the following equation that is due to conservation of current through setting its divergence to zero:

$$\nabla^2\phi=\nabla\cdot(\vec{V}\times\vec{B}) \tag{3}$$

For the problem here, it becomes:

$$\nabla^2\phi=0 \tag{4}$$

With two insulating walls and other walls (i.e., electrodes) subject to a potential difference, the electric potential distribution leads to the generation of a constant electric field. Now, the electrical field can be coupled with the magnetic field with $E_z=-KU_mB$, and $0<K<1$ [39].

GOVERNING EQUATIONS AND BOUNDARY CONDITIONS

The governing equations related to the steady, incompressible, two-dimensional electromagneto-hydrodynamic flows are as the following:

$$\frac{\partial U}{\partial X}+\frac{\partial V}{\partial Y}=0 \tag{5}$$

$$-\frac{\partial P}{\partial X}+\mu\frac{\partial^2 U}{\partial Y^2}-\sigma B(E_z+BU)=0 \tag{6}$$

$$\rho c_p U\frac{\partial T}{\partial X}=k\left(\frac{\partial^2 T}{\partial Y^2}\right)+\sigma E_z(E_z+BU)+\alpha\mu\left(\frac{\partial U}{\partial Y}\right)^2 \tag{7}$$

Lorentz force and joule heating source terms, which are added to the momentum and the energy equations, respectively, enable one to simulate the flow exposed to electromagnetic field. Similar to the mentioned source terms, the viscous dissipation term is also attached to the energy equation. The first model of slippage at walls, suggested by Navier [42] who assumed that the velocity at a solid surface is proportional to the shear stress at the surface, is considered here:

$$U_s - U_w = \frac{2-\sigma_v}{\sigma_v} l \left(\frac{\partial U}{\partial Y}\right)_w \tag{8}$$

Here, tangential momentum accommodation coefficients, σ_v, is assumed to be unity.

Analytical solutions can be greatly facilitated by non-dimensionalizing. The parameters below are used for this purpose:

$$u = \frac{U}{U_m} \quad v = \frac{V}{U_m} \quad y = \frac{Y}{D} \quad x = \frac{X}{D} \quad p = \frac{P}{\rho U_m^2}$$

The following non-dimensional numbers are also used for non-dimensionalizing:

$$Ha^2 = \frac{\sigma}{\mu} B^2 D^2 \quad Re = \frac{\rho U_m D}{\mu} \quad L = \frac{l}{D}$$

Where, Ha is Hartmann number, Re is Reynolds number, and L is dimensionless slip length. For all parameters used in this paper, refer to the Nomenclature. The dimensionless continuity, momentum and the slip boundary condition according to the parameters and the non-dimensional numbers take the following form:

$$\frac{\partial u}{\partial x} + \frac{\partial v}{\partial y} = 0 \tag{9}$$

$$\frac{\partial^2 u}{\partial y^2} - Ha^2 u = Re \frac{\partial p}{\partial x} - K Ha^2 \tag{10}$$

$$u_s - u_w = L \left(\frac{\partial u}{\partial y}\right)_{y=0} \tag{11}$$

Here, the non-dimensional parameter y varies in the range of 0<y< 0.5. Subscripts s and w in all equations denote to the fluid properties at the wall and the wall, respectively. Note that the related energy equation will be presented in the following section.

ANALYSIS

The non-dimensionalized energy equation is solved theoretically to obtain the characteristics of convective heat transfer in parallel plate microchannels in the absence of axial conduction. Under the slip condition at walls, the fluid develops a velocity profile pertinent to electromagneto-hydrodynamic slip flow, which is taken from prior work [40]:

$$u = \left(-\frac{\partial p}{\partial x} Re + K\ Ha^2\right) \left(\frac{-\cosh\left(Ha\left(y-\frac{1}{4}\right)\right)}{Ha^2 \xi} + \frac{1}{Ha^2}\right) \tag{12}$$

or

$$u = \frac{Ha}{-4\sinh\left(\frac{Ha}{4}\right) + Ha\,\xi} \left(-\cosh\left(Ha\left(y-\frac{1}{4}\right)\right) + \xi\right) \tag{12a}$$

where

$$\xi = \cosh\left(\frac{Ha}{4}\right) + Ha\ L\ \sinh\left(\frac{Ha}{4}\right) \tag{13}$$

and

$$\frac{\partial p}{\partial x} = \frac{Ha^3 \xi (1-K) + 4\ K\ Ha^2 \sinh\left(\frac{Ha}{4}\right)}{Re\left(4\sinh\left(\frac{Ha}{4}\right) - Ha\,\xi\right)} \tag{13a}$$

Here, for facilitating, let λ to be defined as:

$$\lambda = \frac{Ha}{-4\sinh\left(\frac{Ha}{4}\right) + Ha\,\xi} = \left(-\frac{\partial p}{\partial x} Re + K\ Ha^2\right) \tag{14}$$

Therefore, the velocity profile reads:

$$u = \lambda \left(-\cosh\left(Ha\left(y-\frac{1}{4}\right)\right) + \xi\right) \tag{15}$$

The way of making temperature dimensionless appropriate to the energy equation in the case of isoflux walls is taken different from that of Shojaeian and Shojaeian [40] to avoid a misinterpretation of the relevant $\partial T/\partial X$ due to the inclusion of viscous dissipation. The energy equation in dimensional form is as:

$$\rho c_p U \frac{\partial T}{\partial X} = k \frac{\partial^2 T}{\partial Y^2} + \sigma E_z (E_z + BU) + \alpha \mu \left(\frac{\partial U}{\partial Y}\right)^2 \tag{16}$$

In the present work, α=0 refers to the absence of the viscous dissipation, while α=1 is pertinent to its presence. The longitudinal temperature gradient in the fully developed region appeared in Eq. (16), $\partial T/\partial X$, is unknown and can be acquired by carrying out an overall energy balance for an elemental control volume, which in general form is written as:

$$\dot{m} c_p \frac{\partial T}{\partial X} = q'' P + \int \mu \phi \, dS \tag{17}$$

Therefore, for the present case it should read:

$$\rho U_m H c_p \frac{\partial T}{\partial X} = q'' \left(2 + \frac{1}{q''} \int_0^H \sigma E_z (E_z + BU) dY + \alpha \frac{\mu}{q''} \int_0^H \left(\frac{\partial U}{\partial Y}\right)^2 dY\right) \tag{18}$$

By non-dimensionalizing along with employing the Brinkman number, defined as $Br=(\mu U_m^2/Dq'')$, and doing the integral on the right-side, one finds:

$$\frac{\partial T}{\partial X} = \frac{q'' A}{\rho U_m H c_p} \tag{19}$$

where A is:

$$A = 2 + \int_0^{0.5} (-K(BrH_a^2)(-K+u)) dy + \alpha Br \int_0^{0.5} \left(\frac{\partial u}{\partial y}\right)^2 dy \tag{20}$$

Now, $\partial T/\partial X$ in Eq. (16) can be substituted with Eq. (19). Defining $\theta=(T-\overline{T}_w)/(Dq''/k)$, one gets to the following dimensionless thermal energy equation:

$$2Au = \frac{\partial^2 \theta}{\partial y^2} - KBrHa^2(-K+u) + \alpha Br \left(\frac{\partial u}{\partial y}\right)^2 \tag{21}$$

The following thermal boundary conditions including non-tempera-

ture jump and asymmetry are applied:

$$\theta(y=0)=0,\ \partial\theta/\partial y\ (y=0.25)=0 \tag{22}$$

Thus, a solution for the energy equation is obtained as:

$$\theta=\frac{T-\overline{T}_w}{Dq''/k}=\left(\frac{\lambda(A+2BrKHa^2)}{Ha^2}-\frac{2BrK^2}{\xi}\right)\left(2\cosh\left(\frac{Ha}{4}\right)-2\cosh\left(\frac{Ha(4y-1)}{4}\right)+\xi Ha^2\left(y^2-\frac{y}{2}\right)\right)+\frac{BrK^2}{\xi}\left(\cosh\left(\frac{Ha}{4}\right)-\cosh\left(\frac{Ha(4y-1)}{4}\right)\right)+\alpha\left(\frac{Br\lambda^2}{8}\right)\left\{\cosh\left(\frac{Ha}{2}\right)-\cosh\left(\frac{Ha(4y-1)}{2}\right)+2Ha^2\left(y^2-\frac{y}{2}\right)\right\} \tag{23}$$

Furthermore, one needs to have dimensionless bulk or mean temperature, which is given by:

$$\theta_m=\frac{\int u\theta dS}{\int u dS} \tag{24}$$

So the corresponding dimensionless mean temperature is derived as:

$$\theta_m=\frac{T_m-\overline{T}_w}{Dq''/k}=\frac{\lambda^2(2A+BrKHa^2)C_1-\lambda BrK^2Ha^2C_2+\alpha BrHa^2\lambda^3C_3}{-96Ha^3} \tag{25}$$

where

$$C_1=768\xi\sinh\left(\frac{Ha}{4}\right)-192\xi Ha\cosh\left(\frac{Ha}{4}\right)+96\sinh\left(\frac{Ha}{2}\right)+2\xi^2Ha^3-48Ha$$

$$C_2=384\sinh\left(\frac{Ha}{4}\right)-96Ha\cosh\left(\frac{Ha}{4}\right)+2\xi Ha^3 \tag{26}$$

$$C_3=144\sinh\left(\frac{Ha}{4}\right)-48Ha\cosh\left(\frac{Ha}{4}\right)+16\sinh\left(\frac{3Ha}{4}\right)+24\xi\sinh\left(\frac{Ha}{2}\right)+\xi Ha^3-12\xi Ha\cosh\left(\frac{Ha}{2}\right)$$

A is also obtainable from Eq. (20) as:

$$A=2+2KBrHa\lambda\sinh\left(\frac{Ha}{4}\right)-\frac{KBrHa^2\lambda\xi}{2}+\frac{BrK^2Ha^2}{2}+\alpha\frac{BrHa\lambda^2}{4}\left\{-Ha+4\sinh\left(\frac{Ha}{4}\right)\cosh\left(\frac{Ha}{4}\right)\right\} \tag{27}$$

Therefore, the Nusselt number, which is normally defined as $Nu=(Dq'')/(k(\overline{T}_w-T_m)$, is written in non-dimensional form as:

$$Nu=\frac{-1}{\theta_m} \tag{28}$$

Finally, for a fully developed laminar microflow, the Nusselt number takes the following form:

$$Nu=\frac{96Ha^3}{\lambda^2(2A+BrKHa^2)C_1-\lambda BrK^2Ha^2C_2+\alpha BrHa^2\lambda^3C_3} \tag{29}$$

Table 1. Nusselt number for fully developed flow between parallel plates with isoflux walls for Ha=4 and K=0.5

L	0		0.01		0.1	
Br	Case I	Case II	Case I	Case II	Case I	Case II
−0.1	8.464	8.480	8.787	8.803	10.243	10.252
−0.01	8.333	8.333	8.665	8.665	10.168	10.168
−0.001	8.320	8.320	8.653	8.653	10.161	10.161
0.001	8.317	8.317	8.650	8.650	10.159	10.159
0.01	8.304	8.304	8.638	8.638	10.152	10.152
0.1	8.178	8.190	8.519	8.531	10.078	10.085

The validation is conducted by a comparison with the previous paper [40] in the case where viscous dissipation and temperature-jump are absent with Ha=4 and K=0.5. Table 1 verifies that present results (Case I) are in complete agreement with those of Ref. [40] (Case II), although some trivial deviations are observed for high Brinkman number owing to the different definition for dimensionless temperature. Note that parameter A given by Shojaeian and Shojaeian [40] should be assumed 4 for the comparison.

RESULTS AND DISCUSSION

This section represents the influences of the slippage and the electromagnetic field on the heat transfer rate for the hydrodynamically and thermally fully developed liquid metal flow inside parallel plate microchannels with isoflux walls, while the viscous dissipation is also taken into consideration. The following results are based on a different dimensionless temperature and a modified longitudinal temperature gradient compared to the recent paper [40], as mentioned before. It is worth noting that the current work can be generalized to mini- and macro-scale flows through setting the slippage parameter, L, to zero. Viscous dissipation as a source term in the energy equation converts kinetic motion of the fluid to thermal energy and

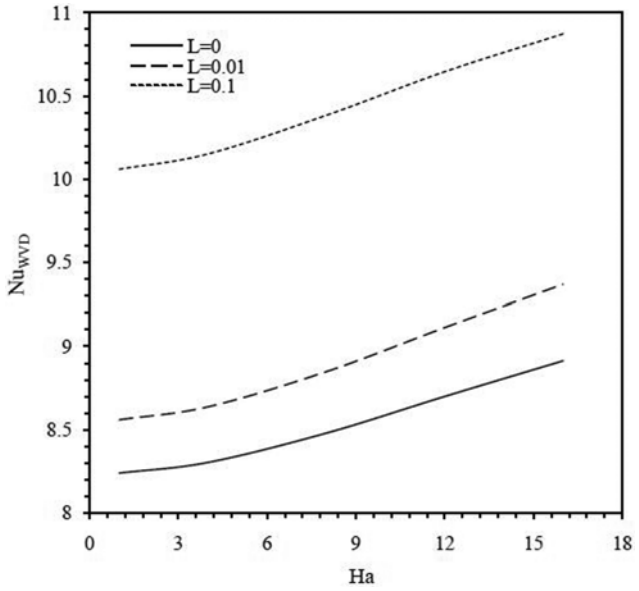

Fig. 2. Variation of fully developed Nusselt number versus Ha for different values of L at Br=0.01, K=0.5 and α=0.

gives rise to a change in the temperature distribution. Again, it is worth noting that $\alpha=0$ indicates the case where the viscous dissipation is ignored, in contrary with $\alpha=1$ for taking it into consideration. Fig. 2 shows the variation of Nusselt number versus Hartmann number for different L at Br=0.01 and K=0.5 with taking no viscous dissipation, denoted by Nu_{WVD}. As expected, the Nusselt number moderately increases with increasing the effect of electromagnetic field (i.e. Ha) in the range within about 8.1% for L=0.1 and 8.2% for L=0 at the given conditions. This behavior is because the velocity-slip increases with Hartmann number for a fixed L, according to Eq. (12a). In other words, if L is kept to be constant, an increase in the velocity-slip, as a consequence of applying stronger electromagnetic field, enhances the rate of heat transfer since it augments advection near walls where diffusion is dominant. In a sense, an increment in Ha through using a stronger magnet causes the fluid particles near wall to have more movement, which facilitates convective heat transfer. The slippage is also analogous to a magnet in influencing the fluid particles motion adjacent to walls.

In Fig. 3, the normalized Nusselt number, Nu_{NORM}, defined as the ratio of the Nusselt numbers for the two cases where the viscous dissipation is included (i.e., $\alpha=1$) and where the viscous dissipation is ignored by setting $\alpha=0$, is depicted versus Hartmann number for different L at K=0.5 and Br=0.01. The Brinkman number in the analysis comes from both the electromagnetic field and the viscous dissipation effects. It is well-known that the positive values of Br correspond to the wall heating (fluid is being heated by walls), and negative values refer to the wall cooling. As seen in the figure, it is obvious that the inclusion of viscous dissipation decreases the Nusselt numbers in the case of wall heating. The reason is that the viscous dissipation always contributes to internal heating of the fluid, and accordingly, for Br>0 the temperature difference, regarded as a factor for transferring the heat from the wall into the fluid, increases as a result and leads to the Nusselt number to be lessened, as expected from Eq. (28). Note that the variation trend of the Nusselt number with Ha under the influence of viscous dissipation, denoted by Nu_{VD}, is similar to that of Nu_{WVD}. Furthermore, the decreasing trend of Nu_{NORM} with Ha, observed in Fig. 3, for those related to low L is more than that of high L. In other words, the convective heat transfer is less sensitive to viscous heating at high slippage since more slippage on the wall gives rise to the decrease of the velocity gradient at the wall. Subsequently, this reduction undermines the impact of the viscous dissipation term. For example, for Ha=16, L=0.1, Br=0.01 and K=0.5, ignoring the viscous dissipation has a negligible effect on the Nusselt number, compared to 10% overestimation with the same condition but for L=0.

In Figs. 4 and 5, the values of Nu_{WVD} and Nu_{NORM} are plotted as a function of Ha for different K at L=0.01 and Br=0.01. The figures explain that with the increase of Ha the heat transfer rate enhances for a fixed K, as mentioned before. One can observe that ignoring

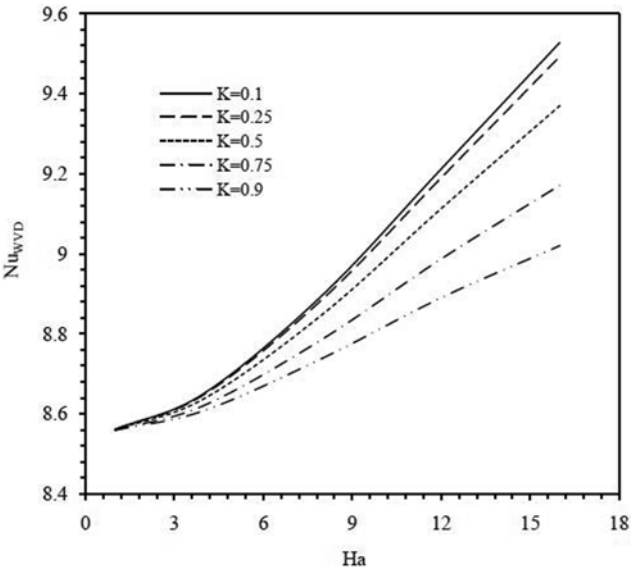

Fig. 4. Variation of fully developed Nusselt number as function of Ha for different K at Br=0.01, L=0.01 and $\alpha=0$.

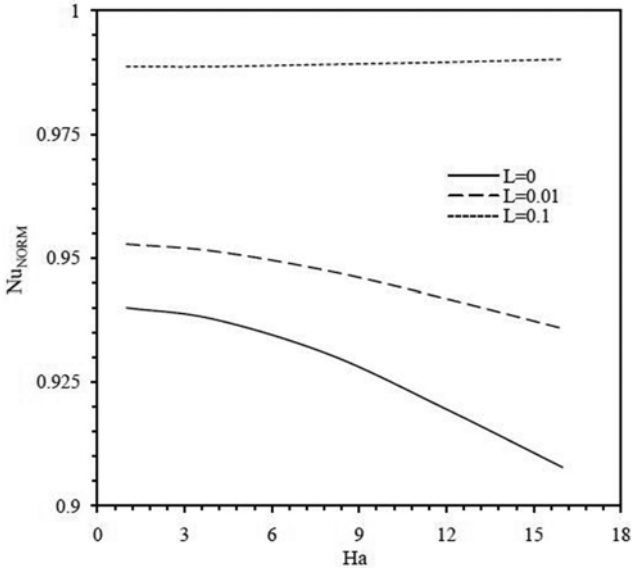

Fig. 3. Variation of fully developed normalized Nusselt number versus Ha for different values of L at Br=0.01, K=0.5 and $\alpha=1$.

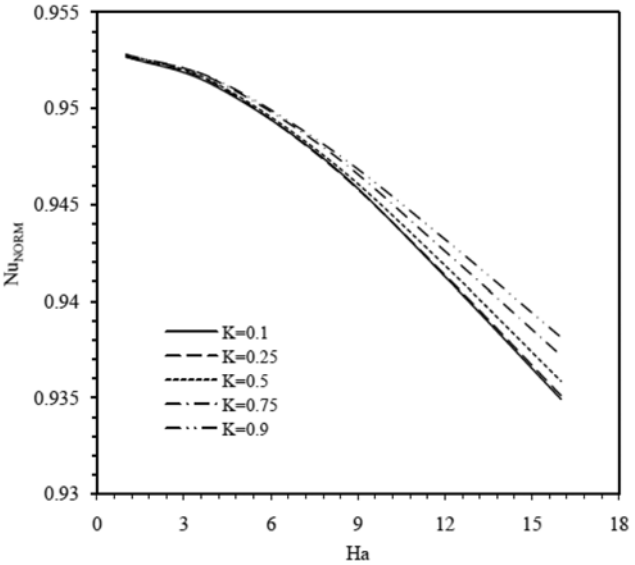

Fig. 5. Variation of fully developed normalized Nusselt number as function of Ha for different K at Br=0.01, L=0.01 and $\alpha=1$.

the viscous heating also overrates the Nusselt number in this case, according to Fig. 5. Also, both Nu_{WVD} and Nu_{VD} vary roughly 5% when K goes from 0.1 to 0.9 for Ha=16, while their variation with K is almost none at Ha=1. In other words, the change in K, which proportionally links the electric and the magnetic fields, is effective for the heat transfer rate if a strong magnetic field applies on the fluid.

The effect of Br on the Nusselt number for various Ha at K=0.5 and L=0.01 is shown in Fig. 6, while the viscous dissipation is neglected (i.e., Nu_{WVD}). One can find that, except for very low Ha in which Br does not change the rate of heat transfer, the value of Nu_{WVD} decreases with the increase of Br in the case of wall heating (Br>0). In contrast, Nu_{WVD} is enhanced with increasing Br in negative direction when the fluid is being cooled (Br<0). These behaviors can be ascribed to the fact that for wall heating case, in a similar manner that the viscous dissipation acts, the increasing Br leads to an increase in the temperature difference between the mean (bulk) fluid and the wall. Therefore, it makes the Nusselt number to be decreased. On the other hand, for wall cooling (Br<0), increasing Br in the negative direction leads to the augmentation of the heat transfer rate by decreasing the temperature difference more. Fig. 7 gives the variation of the normalized Nusselt number, Nu_{NORM}, as a function of Ha at different Brinkman numbers for K=0.5 and L=0.01. The results reveal that neglecting the effect of viscous dissipation overestimates the value of the Nusselt number for wall heating, as expected. For instance, it is about 6.8% for Br=0.01 and Ha=16, compared to the wall cooling case in which the heat transfer rate is underestimated nearly 7.1% for Br=−0.01. Besides, it is found from Figs. 6 and 7 that the contribution of the electromagnetic field to the convection for Br<0 is more than Br>0. Moreover, with Br going toward infinity for either wall heating or wall cooling, the Nusselt number approaches the asymptotic value of Nu=0, as expected from Eq. (29). This is because the heat generated internally by the joule heating and the viscous dissipation reaches a balance with the influence of wall heating or cooling, resulting in a thermal equilibrium state.

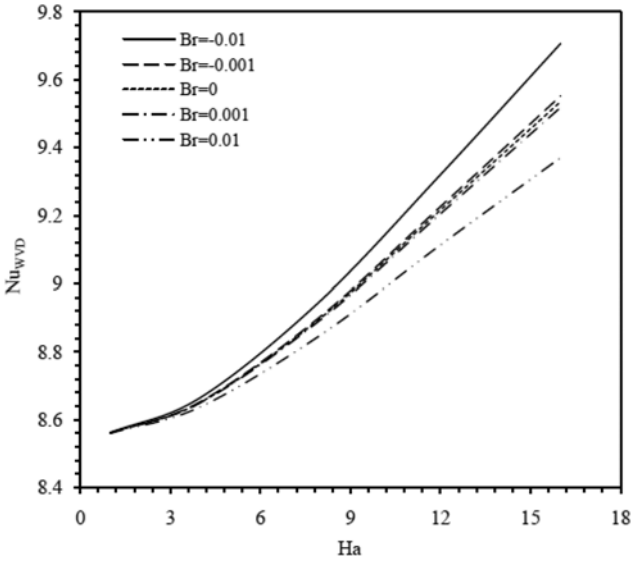

Fig. 6. Variation of fully developed Nusselt number as function of Ha for different Br at K=0.5, L=0.01 and α=0.

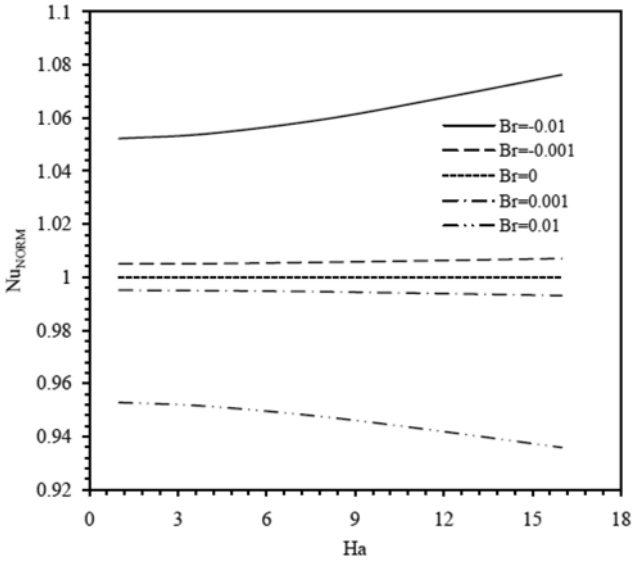

Fig. 7. Variation of fully developed normalized Nusselt number as function of Ha for different Br at K=0.5, L=0.01 and α=1.

The variations of Nu_{WVD} and Nu_{VD} with respect to dimensionless slip length at different Br at K=0.5 and Ha=4 are given in Tables 2 and 3. It is understood from the tables that the value of Nu_{WVD} has a very little change with Br, whereas the viscous heating gives rise to the heat transfer rate to be changed under the influence of Br, especially when the fluid is subject to a less slippage. For instance, a change in Br from −0.01 to 0.01 causes a nearly 10% decline in Nu_{VD} for L=0.01, while the decline is about 1.3% at L=0.1. This can be attributed to the notion that the slippage, which tends to unify the velocity profile, leads to smaller velocity gradients and subsequently smaller shear rates, causing a decline in the viscous heating effect.

The variations of singular values of Br with Hartmann number

Table 2. Fully developed Nusselt number without considering viscous dissipation at K=0.5 and Ha=4

	Br				
	−0.01	−0.001	0	0.001	0.01
L					
0	8.333	8.32	8.318	8.317	8.304
0.01	8.665	8.653	8.651	8.65	8.638
0.1	10.168	10.161	10.16	10.159	10.037
1	11.669	11.668	11.667	11.667	11.666

Table 3. Fully developed Nusselt number with viscous dissipation included at K=0.5 and Ha=4

	Br				
	−0.01	−0.001	0	0.001	0.01
L					
0	8.927	8.375	8.318	8.262	7.787
0.01	9.133	8.697	8.651	8.606	8.218
0.1	10.285	10.172	10.160	10.147	10.152
1	11.672	11.668	11.667	11.667	11.662

Table 4. Singular values of Brinkman number at K=0.5

	Ha	1	4	8	12	16
L	α=0					
0		−90.895	−5.815	−1.558	−0.762	−0.476
0.01		−100.328	−6.464	−1.762	−0.883	−0.568
0.1		−186.668	−12.339	−3.610	−1.976	−1.390
	α=1					
0		−0.157	−0.147	−0.123	−0.099	−0.080
0.01		−0.201	−0.190	−0.163	−0.136	−0.115
0.1		−0.865	−0.821	−0.725	−0.640	−0.580

at different L are shown in Table 4. In singular points, the heat transfer cannot be stated in terms of Nusselt number, but it can be expressed that the heat transferred between the wall and the mean fluid gets to a balance with the internal heat generation caused by the viscous dissipation and the joule heating. Opposite to the slippage, for either applying a stronger electromagnetic field or including the viscous dissipation, the singularity points render toward a smaller value of Br with negative sign.

At the end, If interested to obtain the Nusselt number when the flow is under the sole influence of electromagnetic force, it is sufficient to leave out the pressure gradient term $\partial p/\partial x$ appearing in Eq. (14) by setting it to zero and substituting λ=K Ha^2 into the Nusselt number expression.

CONCLUSIONS

An analytical investigation of both hydrodynamically and thermally fully developed forced convection under the influences of electromagnetic field and slippage has been carried out for flow inside parallel plate microchannels in the case of isoflux walls. In addition to the slip wall boundary condition, the electromagnetic field via the two source terms, Lorentz force into the momentum equation and Joule heating into the energy equation, have been fulfilled in the analysis. The interactive effects among the Hartmann number, Brinkman number and dimensionless slip length on the heat transfer characteristics have been examined in detail. It has been observed that increasing the electromagnetic field totally causes the augmentation of the Nusselt number. The alteration of the Nusselt number with the Brinkman number has shown some singularities for each L that becomes closer when viscous dissipation is included. Furthermore, the results have demonstrated that the heat transfer rate may be overestimated or underestimated owing to neglecting the viscous heating, which depends on the case of the fluid in terms of wall heating or wall cooling. Therefore, the effect of the viscous dissipation on the convective heat transfer, for liquid flows through parallel plate microchannels, under the influence of electromagnetic field is significant to deal with.

NOMENCLATURE

A : constant obtained by Eq. (27)
B : magnetic field strength
Br : Brinkman number
C_1, C_2, C_3 : constant defined in Eq. (26)
c_p : specific heat at constant pressure
D : hydraulic diameter
E : electric field strength
H : height of channel
Ha : hartmann number
k : thermal conductivity of fluid
K : $-E/(U_m B)$
L : dimensionless slip length
l : mean free path
$\dot{m}$: mass flow rate
Nu : nusselt Number
Nu_{WVD} : nusselt Number in absence of viscous dissipation
Nu_{VD} : nusselt Number in presence of viscous dissipation
p : pressure
q'' : heat flux
Re : Reynolds number
Re_m : magnetic Reynolds number, $\mu_m U_m L$
S : cross-section area
T : temperature
U, V : dimensional velocity component in the x, y directions
u, v : dimensionless velocity component in the x, y directions
U_m : mean velocity
W : width of channel
X, Y : dimensional position in coordinate system
x, y : dimensionless position in coordinate system

Greek Symbols

α : constant that takes 1 for including viscous dissipation and 0 for neglecting viscous dissipation
γ : specific heat ratio of fluid
λ : constant defined by Eq. (14)
μ : dynamic viscosity of fluid
μ_m : magnetic permeability
ξ : constant defined by Eq. (13)
ρ : density of fluid
θ : dimensionless temperature
σ : electric conductivity
σ_v : tangential momentum accommodation coefficient
σ_T : thermal accommodation coefficient

Subscripts

i : fluid properties at the inlet
m : mean or bulk
s : fluid properties at the wall
w : wall

REFERENCES

1. D. K. Bailey, T. A. Ameel, R. O. Warrington and T. I. Savoie, Proceedings of the IECEC Conference, ES-396, ASME-FL, Orlando (1995).
2. A. B. Duncan and G. P. Peterson, *Appl. Mech. Rev.*, **47**, 397 (1994).
3. G. L. Morini, *Int. J. Therm. Sci.*, **43**, 631 (2004).
4. M. S. Chun and S. Lee, *Colloids Surf. A*, **267**, 86 (2005).
5. P. Joseph and P. Tabeling, *Phys. Rev. E*, **71**, 035303(R) (2005).
6. D. C. Tretheway and C. D. Meinhart, *Phys. Fluids*, **14**, 9 (2002).
7. M. El-Genk and I. Yang, *J. Heat Trans.-ASME*, **130**, 082405-1

(2008).
8. H. P. Kavehpour, M. Faghri and Y. Asako, *Numer. Heat Trans. Part A*, **32**, 677 (1997).
9. G. D. Ngoma and F. Erchiqui, *Int. J. Therm. Sci.*, **46**, 1076 (2007).
10. M. Shams, M. Shojaeian, C. Aghanajafi and S. A. R. Dibaji, *Int. Commun. Heat Mass Trans.*, **36**, 1075 (2009).
11. M. Shojaeian and S. A. R. Dibaji, *Int. Commun. Heat Mass Trans.*, **37**, 324 (2010).
12. B. Xu, K. T. Ooi, C. Mavriplis and M. E. Zaghloul, *J. Micromech. Microeng.*, **13**, 53 (2003).
13. T. N. Aynur, L. Kuddusi and N. Eğrican, *Heat Mass Trans.*, **42**, 1093 (2006).
14. C. H. Chen, *Heat Mass Trans.*, **42**, 853 (2006).
15. K. Hooman, *Int. Commun. Heat Mass Trans.*, **34**, 945 (2007).
16. J. Koo and C. Kleinstreuer, *J. Micromech. Microeng.*, **13**, 568 (2003).
17. J. Koo and C. Kleinstreuer, *Int. J. Heat Mass Trans.*, **47**, 3159 (2004).
18. J. V. Rij, T. Ameel and T. Harman, *Int. J. Therm. Sci.*, **48**, 271 (2009).
19. A. Sadeghi and M. H. Saidi, *J. Heat Trans.-ASME*, **132**, 072401 (2010).
20. C. P. Tso and S. P. Mahulikar, *Int. J. Heat Mass Trans.*, **41**, 1759 (1998).
21. R. A. Alpher, *Int. J. Heat Mass Trans.*, **3**, 108 (1961).
22. M. Ghassemi, H. Rezaeinezhad and A. Shahidian, *Proceedings of 14th symposium on electromagnetic launch technology*, June, Victoria, 1-4 (2008).
23. R. C. Gupta, *Mech. Res. Commun.*, **19**, 73 (1992).
24. S. L. L. Verardi, J. M. Machado and J. R. Cardoso, *IEEE Transaction Magnetics*, **38**, 941 (2002).
25. O. Andreev, Y. Kolesnikov and A. Thess, *Phys. Fluids*, **18**, 065108 (2006).
26. O. Andreev, Y. Kolesnikov and A. Thess, *Exp. Fluids*, **46**, 77 (2009).
27. H. Chen, T. Zhoub, Z. Yangb, R. Lüb, Z. Zhub and M. Ni, *Fusion Eng. Des.*, **85**, 1742 (2010).
28. H. Duwairi and M. Abdollah, *Microsyst. Technol.*, **13**, 33 (2007).
29. J. Jang and S. S. Lee, *Sensor. Actuat. A*, **80**, 84 (2000).
30. A. V. Lemoff and A. P. Lee, *Sensor. Actuat. B*, **63**, 178 (2000).
31. P. J. Wang, C. Y. Chang and M. L. Chang, *Biosens. Bioelectron.*, **20**, 115 (2004).
32. A. C. Siegel, D. A. Bruzewicz, D. B. Weibel and G. M. Whitesides, *Adv. Mater.*, **19**, 727 (2007).
33. A. C. Siegel, S. S. Shevkoplyas, D. B. Weibel, D. A. Bruzewicz, A. W. Martinez and G. M. Whitesides, *Angew. Chem. Int. Ed.*, **45**, 6877 (2006).
34. M. D. Dickey, R. C. Chiechi, R. J. Larsen, E. A. Weiss, D. A. Weitz and G. M. Whitesides, *Adv. Funct. Mater.*, **18**, 1097 (2008).
35. S. Z. Qian and H. H. Bau, *Mech. Res. Commun.*, **36**, 382 (2009).
36. V. M. Soundalgekar, *Proc. Natl. Inst. Sci. India Part A*, **33**, 276 (1967).
37. V. M. Soundalgekar, *Proc. Natl. Inst. Sci. India Part A*, **135**, 251 (1969).
38. V. M. Soundalgekar, *Proc. Natl. Inst. Sci. India Part A*, **35**, 439 (1969).
39. C. Cai and D. Liu, *AIAA J.*, **47**, 542 (2009).
40. M. Shojaeian and M. Shojaeian, *Microfluid. Nanofluid.*, **12**, 553 (2012).
41. R. K. Agarwal, Proceedings of 36th AIAA Plasmadynamics and Lasers Conference, AIAA, Toronto, 2005-4782 (2005).
42. C. L. M. H. Navier, *Mem. Acad. R. Sci. Inst., France*, **1**, 414 (1823).